International Journal of Engineering and Advanced Technology (IJEAT)
ISSN: 2249-8958 (Online), Volume-9 Issue-2, December, 2019

Transition Metal Oxide-Based Perovskite Structures as A Bifunctional Oxygen lectrocatalysts: Fe Doped Lacoo$_3$ Nanoparticles

Shaik Mahammad Rafi

Abstract: ***In this report, we have investigated lanthanum cobalt iron ($LaCo_{1-x}Fe_xO_3$) perovskite nanoparticles synthesized by combining metallic nitrates, deionized water, and citric acid by using sol-gel method and subsequently calcinated at 400 °C for 1h and 900 °C for 7h, respectively. The formation of single-phase perovskite structure is a series of $LaCo_{1-x}Fe_xO_3$ (x = 0, 0.2, 0.4, 0.6, 0.8, 1). The crystal structure, mean particle, and morphology properties of the prepared $LaCo_{1-x}Fe_xO_3$ perovskite oxide nanoparticles were examined by X-ray diffraction (XRD), field emission scanning electron microscopy (FESEM). The perovskite structure has shown special performance for oxygen reduction reaction (ORR) and oxygen evolution reaction (OER) catalytic activity in alkaline medium. As the combined valence transition metal oxides are rising capable candidates for bifunctional electrocatalysts, the electrochemical performance of the $LaCo_{1-x}Fe_xO_3$ catalyst was thoroughly investigated. Koutecky-Levich results on the ORR polarization curves of all compounds shows that the four-electron pathway is favorable on these perovskite oxides. In this paper, we report B-site Fe doping in perovskite structure is a sufficient strategy to improve ORR and OER catalytic activity for application in metal-air batteries.***

Keywords: ***Metal-air batteries, Bifunctional catalyst, Perovskite oxides, Electrochemical behavior.***

I. INTRODCTION

Due to technological developments, people's demand, safety, clean, and renewable energy sources have been required considerable attention over the years. Also, rechargeable metal-air batteries are considered one of the most exciting technologies owing to its low price, high power density, environmentally friendly [1]. The development of rechargeable metal-air batteries is mostly restricted by two slow mechanisms, notably, the ORR and OER kinetics of oxygen catalyst [2]. Nowadays, Pt and IrO_2 are considered as the standard electrocatalysts about ORR and OER. Nevertheless, the high expensive, disappointing lifetime and limited availability badly limit their practical applications [3,4]. Therefore, the current research on the alternative capable catalysts based on non-precious metal/metal composites, developing low-cost catalyst materials, practically both ORR and OER are active bifunctional electrocatalyst with high demand [5].

Revised Manuscript Received on December 30, 2019.
* Correspondence Author
Shaik Mahammad Rafi, Department of Advanced Materials Engineering, Kongju National University, Cheonan-si, Chungnam 31080, Republic of Korea

Among the different bifunctional catalysts, lanthanum-based perovskite structure is composed of many oxides which are represented by a chemical formula ABO_3. In this case perovskite structure, the A-cation is generally alkaline-earth elements or rare-earth elements on the concerns of the lattice. B-cation on the lattice's concern, which may be transition metal elements. Usually, the metallic A-cation is coordinated by 12 neighboring oxygen ions, similarly altering the insignificant B-cation is coordinated by 6 oxygen ions only. Appropriate substitution of A or B cations can guide to oxygen deficiencies without alternating the basic perovskite structures. ABO_3 perovskite oxides have been applicable as cathode electrocatalysts due to their excellent stability in alkaline solution and high catalytic activity for ORR/OER. In this present work $LaCo_{1-x}Fe_xO_3$ perovskite oxide nanoparticles was synthesized by sol-gel method [6]. $LaCoO_3$ based materials contain very interesting electrocatalytic and electrical properties due to their good ionic conductivity and with high electronic conductivity [7]. Zhu.et.al introducing the effect of A-cation defect into $LaFeO_3$ enhances the best ORR and OER catalytic activity and, therefore, the best bifunctionality. This can be ascribed to the formation of abundant oxygen gaps and a certain amount of the Fe^{4+} species [8]. B-site cation with a reducible primitive transition metal like Mn, Fe, Co provides the activity of the catalytic reaction. Coupling at the B-site leads to the synergetic effect of two different ions, with enhanced electrocatalytic activity. The perovskite oxides activity was associated with redox properties and the high oxygen mobility of the transition metal used [9-11]. However, there has been a significant contribution to the investigation of lanthanum-based perovskite oxide ($LaMO_3$, M = Co, Fe, Mn) in the application of a bifunctional air cathode [12]. This is because, in the present work, we summarized comprehensive research for the sol-gel synthesis of lanthanum-based perovskite oxide $LaCo_{1-x}Fe_xO_3$ nanoparticles and their electro-catalytic activities characterization for ORR and OER reactions.

II. EXPERIMENTAL SECTION

A. Materials

Lanthanum nitrate hexahydrate ($La(NO_3)_3.6H_2O$, 99+%, Aldrich), cobalt nitrate hexahydrate ($Co(NO_3)_2.6H_2O$, 97.7%, Alfa Aesar), iron nitrate nonahydrate ($FeN_3O_9.9H_2O$, 98+%, Alfa Aesar), citric acid anhydrous ($C_6H_8O_7$, 99.5+%, Alfa Aesar), potassium hydroxide (KOH, 85%, Alfa Aesar). These chemicals are used for received without further method.

B. Synthesis of $LaCo_{1-x}Fe_xO_3$ Nanoparticles

For the synthesis of Lanthanum-based nanoparticles, in a series of [$LaCo_{1-x}Fe_xO_3$] (x = 0, 0.2, 0.4, 0.6, 0.8, 1) were synthesized by the sol-gel method. Lanthanum, cobalt, and iron nitrate compounds were dissolved in deionized water. Then added citric acid to the mixed solution. The molar ratio of the metal nitrates and citric acid was set to 1:2. After that, all mixed compound solution was kept stirring with a magnetic stirrer at the temperature of 80 °C. Continue this stirring process until the brown gel formation. Subsequently, these prepared gel samples were placed in a heated furnace at 180 °C to form amorphous precursor, then the dried powder was transferred to a crucible and calcined at 400 °C for 1 h and 900 °C for 7 h. The obtained perovskite structure nanoparticles are $LaCoO_3$, $LaCo_{0.8}Fe_{0.2}O_3$, $LaCo_{0.6}Fe_{0.4}O_3$, $LaCo_{0.4}Fe_{0.6}O_3$, $LaCo_{0.2}Fe_{0.8}O_3$, and $LaFeO_3$.

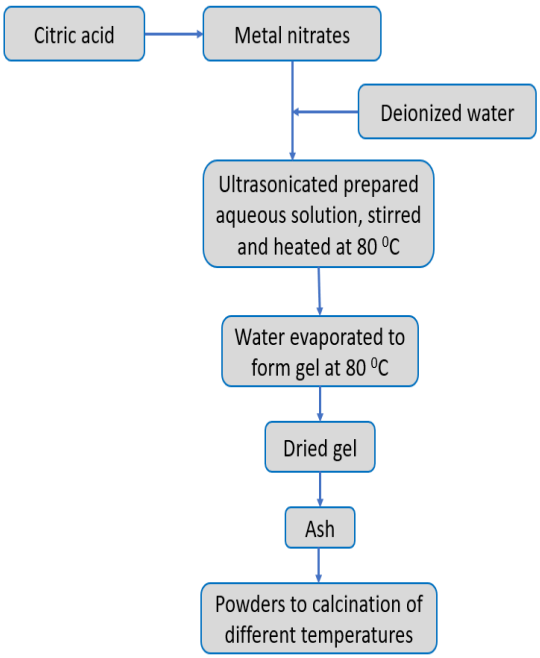

Figure 1. The flow chart shows the fabrication of the $LaCo_{1-x}Fe_xO_3$ compound by the sol-gel method.

C. Characterization Techniques

a. X-ray diffractometer

The crystal structure of synthesized $LaCo_{1-x}Fe_xO_3$ perovskite oxide nanoparticles were characterized by X-ray diffraction (Rigaku Cu Kα radiation with a wavelength of λ = 1.54 Å) technique and 2θ range from 10° to 80°.

b. Field Emission Scanning Electron Microscopy (FESEM)

The mean particle size and morphology of $LaCo_{1-x}Fe_xO_3$ perovskite oxide nanoparticles were characterized by field emission scanning electron microscopy (FESEM) (SIGMA 500, ZEISS) and the distribution of elemental analysis was characterized by energy dispersive spectroscopy (EDS) mapping (Bruker, XFlash 6130).

c. Electrochemical Measurements

The synthesized $LaCo_{1-x}Fe_xO_3$ perovskite oxide nanoparticles for ORR and OER activities, the electrochemical measurements were examined using a rotating ring disk electrode (RRDE) technique connected to the workstation (BAS Inc.). An RRDE is a saturated three-electrode test system for an electrochemical cell, where includes a glassy carbon (GC) substrate diameter of 3.0 mm, a saturated calomel electrode (SCE), and a graphite rod diameter of 6.0 mm. This three-electrode system play a role of reference, working and counter electrodes. The molar ratio of 0.1 M aqueous KOH solution is used as the electrolyte. The catalyst ink solution was prepared by careful mixing of $LaCo_{1-x}Fe_xO_3$ perovskite oxide (2 mg) and Vulcan-XC72 carbon (2 mg) were diluted in 1 mL of ethanol solution mixed with 0.15 mL of Nafion® (perfluorinated resin solution, 5 wt%, Aldrich) by using an ultrasonic cleaner (model: SD200H) to form a homogeneous ink. RRDE glassy carbon disk electrode was earlier polished with a 0.05 μm alumina abrasive suspension (R&B Inc.) on a clean polishing cloth (R&B Inc.) subsequently rinsed with distilled water, and then dried in the oven. After completion of ultrasonication for 1h, 0.36 μL of catalyst ink was coated on to the glassy carbon electrode. Then RRDE experiments and high purity oxygen gas (99.99%) were purged to allow the electrolyte to saturate with oxygen for 30 min. The polarization curves for the oxygen reduction reaction of $LaCo_{1-x}Fe_xO_3$ was tested at the rotation speeds of 500, 1000, 1500, 2000, and 2500 rpm, and oxygen evolution reaction (OER) of $LaCo_{1-x}Fe_xO_3$ at the rotational speed of 1500 rpm, electrolyte using a CHI electrochemical workstation with a scan rate is 0.005 V s^{-1}. The measurements of the electrochemical impedance were carried out with a voltage bias of 5 mV amplitude in the frequency range between 0.1 Hz to 100 kHz. The electron transfer number (n) is the overall reaction was to understand the reaction mechanism of ORR by using the Koutecky-Levich equation:

$$\frac{1}{I} = \frac{1}{I_k} + \frac{1}{I_d} = \frac{1}{nFAkC_{O_2}} + \frac{1}{0.62nFAD_{O_2}^{2/3}\omega^{1/2}\upsilon^{-1/6}C_{O_2}} \quad (1)$$

Where I is the measured current, I_k and I_d are the kinetic and diffusion-limiting current densities, respectively n is the number of electrons exchanged in the reaction, F is the Faraday constant, A is the geometrical surface area (3.1428 × (1.5 mm)^2), k is the rate constant for electron-transfer, Co_2 is the bulk concentration of oxygen dissolved in the electrolyte (1.14×10^{-6} mol cm^{-3}), Do_2 is the diffusion coefficient of oxygen in the bulk solution (1.73×10^{-5} cm^2 s^{-1}), ω is the rotation rate (rad/s), υ is the kinetic viscosity of the electrolyte (0.01 cm^2 s^{-1}).

III. RESULTS AND DISCUSSION

The crystal structure of the synthesized perovskite oxide nanoparticles $LaCo_{1-x}Fe_xO_3$ calcined at 400 °C for 1 h and 900 °C for 7 h were examined by using X-ray diffraction (XRD), as shown in Fig.2(a).

All the samples exhibited the single-phase perovskite cubic crystal structure. Conformed from pure $LaCoO_3$ JCPDS-ICDD file no: 048-0123. No characteristic peaks of lanthanum oxide or cobalt oxide were observed, indicating that the variation of the La/Co molar ratio did not impair the phase structure. Interestingly, we found that there was a clear peak change towards lower 2θ angle (left shift) with increasing of Fe content doping into $LaCoO_3$ such as (0, 0.2, 0.4, 0.6, 0.8, 1) [13].

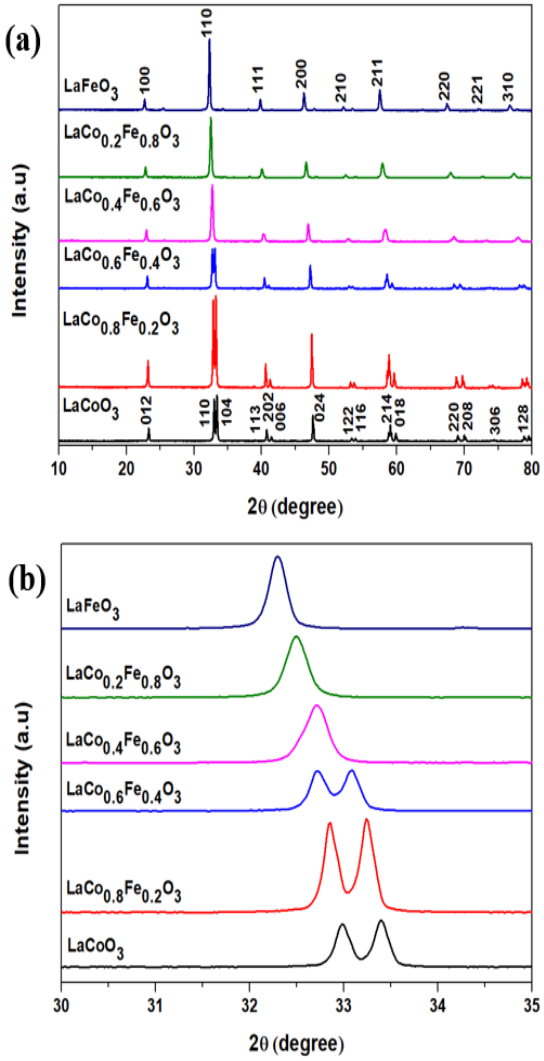

Figure 2. XRD patterns of the (a) $LaCo_{1-x}Fe_xO_3$ over a 2θ range of 10-80°, (b) enlarged XRD peak between 30° and 35°.

The surface morphology of the synthesized $LaCo_{1-x}Fe_xO_3$ perovskite oxide nanoparticles was examined by using field emission scanning electron microscopy (FESEM) as shown in Fig. 3(a-f). The particle size of the corresponding single or double layers has shown several hundreds of nanometers. For instance, the particle size of the components is shown in Fig. 3(a-f) which are 441.3 nm, 641.53 nm, 433.86 nm, 393 nm, 327.83 nm, and 280.53 nm. The particles exhibit random shapes and non-uniform distribution. The modification in sizes of particle probably perovskite attributed to a combination of changes. Fig. 3(g) shows the EDS elemental mapping of perovskite oxide $LaCo_{0.8}Fe_{0.2}O_3$ under FESEM mode which represents the occupancy of 1:1 atomic ratio for La: M (Co, Fe) catalysts. Every chemical element is gradually distributed in the perovskite oxide sample.

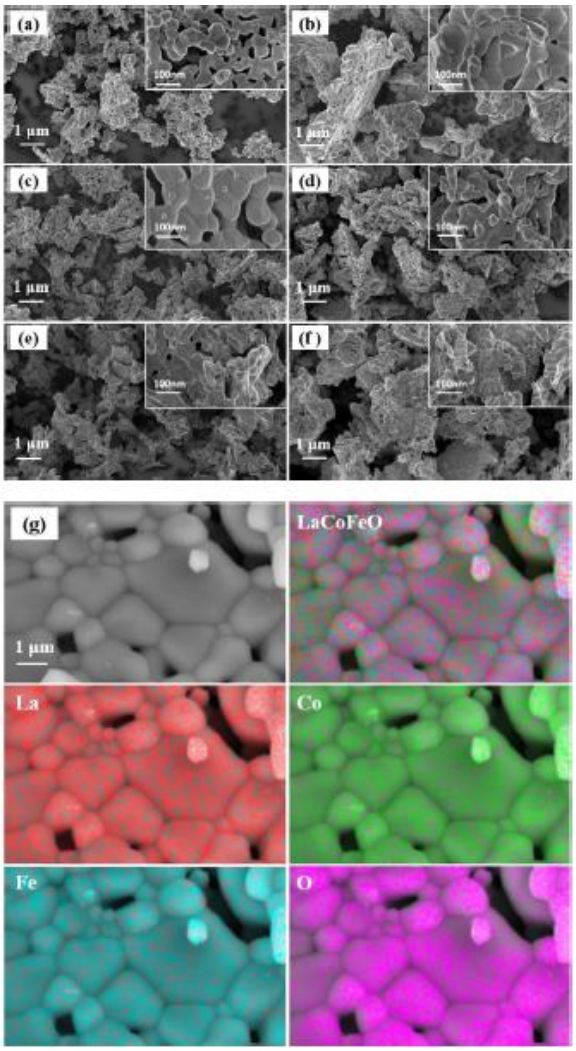

Figure 3. FESEM morphologies of (a) $LaCoO_3$, (b) $LaCo_{0.8}Fe_{0.2}O_3$, (c) $LaCo_{0.6}Fe_{0.4}O_3$, (d) $LaCo_{0.4}Fe_{0.6}O_3$, (e) $LaCo_{0.2}Fe_{0.8}O_3$ and (f) $LaFeO_3$ (the upper right insets show high resolution images), (g) elemental mapping analysis of $LaCo_{0.8}Fe_{0.2}O_3$.

In order to evaluate the activities of the $LaCo_{1-x}Fe_xO_3$ perovskite oxide of the network structure for ORR and OER. Oxygen saturated 0.1 M KOH electrolyte was evaluated in linear sweep voltammetry (LSV) with rotating ring disk electrode (RRDE) measurements with different rotational speeds of 500, 1000, 1500, 2000, and 2500 rpm. Fig. 4(a) shows the $LaCo_{1-x}Fe_xO_3$ perovskite nanoparticles in the ORR current densities of the six samples with a scan rate is 0.005 V s^{-1} under a rotation speed of 1500 rpm in potentials range from -1.0 V to 0.0 V vs. SCE. It indicates the maximum diffusion-limited current density for $LaFeO_3$ that decreases in the sequence of $LaCo_{0.6}Fe_{0.4}O_3$ > $LaCoO_3$ > $LaCo_{0.2}Fe_{0.8}O_3$ > $LaCo_{0.8}Fe_{0.2}O_3$ > $LaCo_{0.4}Fe_{0.6}O_3$. The onset potential of six samples is nearly -0.30 V. The OER operations for models prepared to evaluate their application as bifunctional oxygen electrocatalysts. LSV curves recorded for OER activity in Fig. 4(b) shows an OER explanation of every catalyst in the potential between 0.0 V

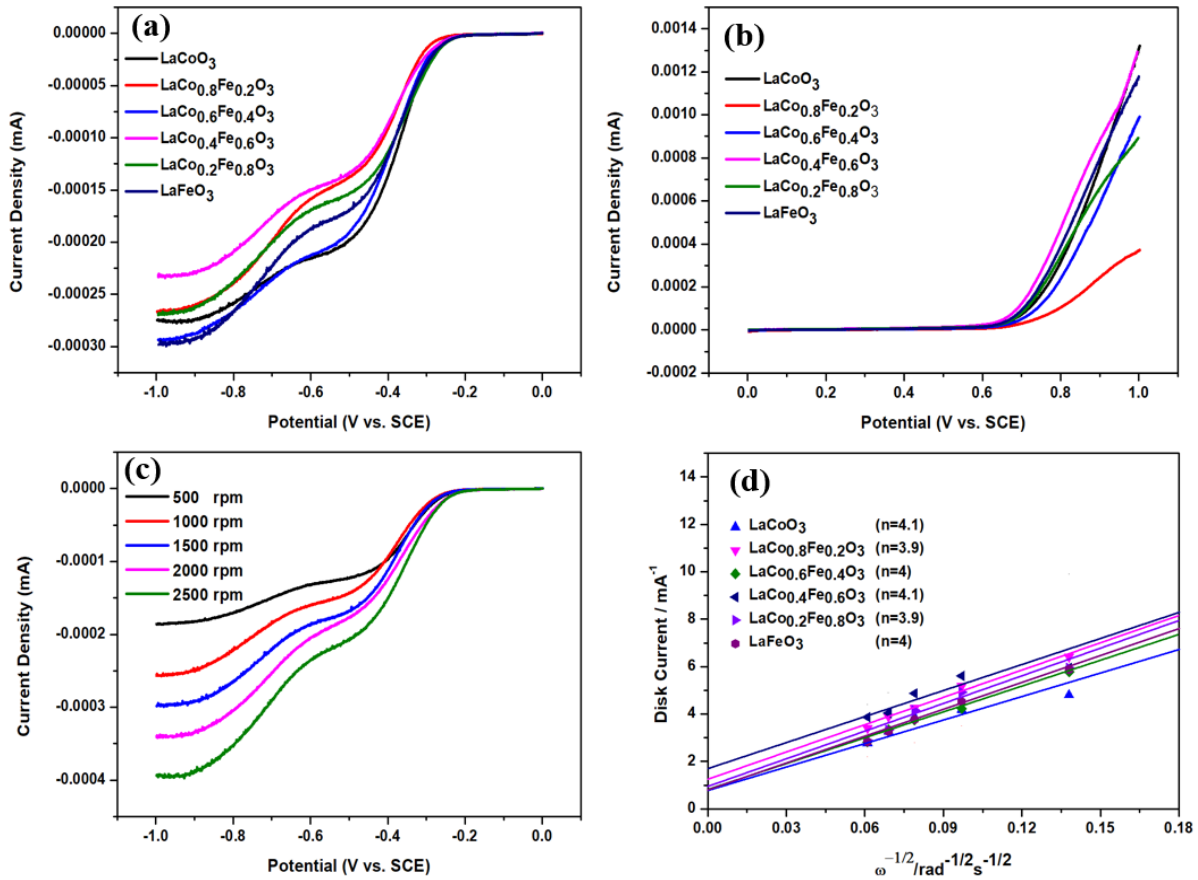

Figure 4. (a) Linear sweep voltammetry (LSV) test on ORR polarization curves at 1500 rpm, (b) OER current densities in the potentials range from 0.0 V to 1.0 V, (c) ORR current density of $LaFeO_3$ at different rotation speeds of 500 to 2500 rpm, (d) Koutecky-Levich analysis of all samples based on ORR curves at -0.80 V.

to 1.0 V vs. SCE. At 0.65 V the kinetics of $LaCo_{0.4}Fe_{0.6}O_3$ is abruptly increasing. The oxygen evolution reaction maximum current density is showing $LaCo_{0.4}Fe_{0.6}O_3$ and decreases in the subsequent order as $LaFeO_3$ > $LaCo_{0.2}Fe_{0.8}O_3$ > $LaCoO_3$ > $LaCo_{0.6}Fe_{0.4}O_3$ > $LaCo_{0.8}Fe_{0.2}O_3$. LSV curves recorded for ORR current density of $LaFeO_3$ on RRDE at different rotational speeds of 500 to 2500 rpm as shown in Fig. 4(c) with the increase in the rotation speed the current density increases that may be owing to rapidly transport dissolved oxygen to the electrode surface [14]. For a more quantitative analysis of the ORR kinetics and electrocatalysts processes by $LaCo_{1-x}Fe_xO_3$ perovskite oxides, we have derived the Koutecky-Levich plots Fig. 4(d) of six samples at -0.80 V vs. SCE from LSV curves based on ORR polarization curves. The electron transfer number (n) can be calculated from the slope of Koutecky-Levich plots by using Eq. (1) for $LaCo_{1-x}Fe_xO_3$ is showing in Fig. 4(d) which are 4.1, 3.9, 4.0, 4.1, 3.9 and 4.0, respectively [5]. All compounds for ORR in alkaline solution are very close to the theoretical value (4.0). The appropriate amount of Fe doping can transmit the ORR mechanism from a 2-electron dominated pathway in the alkaline solution (O_2 toHO_2^-) is the reduction of the 4-electron dominated pathway from O_2 to OH^- [15].

IV. CONCLUSIONS

In summary, $LaCo_{1-x}Fe_xO_3$ was synthesized by using a sol-gel method that decreases the valance state of the surface Co and increases the valance state of the surface Fe. The experimental results indicate the $LaCo_{1-x}Fe_xO_3$ perovskite oxide with cubic crystal structure, there is a clear peak shift towards lower 2θ angle with increasing of Fe content doping into $LaCoO_3$ such as (0, 0.2, 0.4, 0.6, 0.8, 1), and particle size of the corresponding single or double layers has shown several hundreds of nanometers. All the synthesized perovskite oxides were evaluated in 0.1 M KOH electrolyte for electrochemical tests towards ORR and OER. Based on the LSV results, $LaFeO_3$ shows the maximum diffusion-limited current density for ORR. The OER explanation of every catalyst in the potentials range from 0.0 V to 1.0 V vs. SCE. At 0.65 V the kinetics of $LaCo_{0.4}Fe_{0.6}O_3$ is abruptly increasing. Similarly, according to the Koutecky-Levich results on the ORR polarization curves of all compounds indicates a four-electron pathway. Fe-doped $LaCoO_3$ provides a low-cost electrocatalyst for air cathode in metal-air batteries.

ACKNOWLEDGEMENTS

This research was supported by National Research Foundation of Korea (NRF) grant funded by the Korea government (MSIP) (No. 2015R1C1A1A01051733).

REFERENCES

1. R. -H. Yuan, Y. He, W. He, M. Ni, and M. K. H. Leung, "$La_{0.8}Sr_{0.2}MnO_3$ based perovskite with A-site deficiencies as high performance bifunctional electrocatalyst for oxygen reduction and evolution reaction in alkaline," Energy Procedia, vol. 158, Feb. 2019, pp. 5804-5810.
2. R. -H. Yuan, Y. He, W. He, M. Ni, and M. K. H. Leung, "Bifunctional electrocatalytic activity of $La_{0.8}Sr_{0.2}MnO_3$-based perovskite with the A-site deficiency for oxygen reduction and evolution reactions in alkaline media," Applied Energy, vol. 251, Oct. 2019, pp. 113406.
3. G. Nam, J. Park, M. Choi, P. Oh, S. Park, M. G. Kim, N. Park, J. Cho, and J-S. Lee, "Carbon-Coated Core-Shell Fe-Cu Nanoparticles as Highly Active and Durable Electrocatalysts for a Zn-Air Battery," ACS Nano, vol. 9, 2015, pp. 6493-6501.
4. I. S. Amiinu, Z. Pu, X. Liu, K. A. Owusu, H. G. R. Monestel, F. O. Boakye, H. Zhang, and S. Mu, "Multifunctional Mo-N/C@MoS_2 Electrocatalysts for HER, OER, ORR, and Zn-Air Batteries," Advanced Functional Materials, vol. 27, Nov. 2017, pp.1702300.
5. H. Wang, W. Xu, S. Richins, K. Liaw, L. Yan, M. Zhou, and H. Luo, "Polymer-assisted approach to $LaCo_{1-x}Ni_xO_3$ network nanostructures as bifunctional oxygen electrocatalysts," Electrochimica Acta, vol. 296, Feb. 2019, pp. 945-953.
6. U. Megha, K. Shijina, and G. Varghese, "Nanosized $LaCo_{0.6}Fe_{0.4}O_3$ perovskite synthesized by citrate sol gel auto combustion method," Processing and Application of Ceramics, vol. 8, Jan. 2014, pp. 87-92.
7. F. M. Figueiredo, F.M.B. Marques, and J.R. Frade, "Electrochemical permeability of $La_{1-x}Sr_xCoO_{3-\delta}$ materials," Solid State Ionics, vol. 111, Sep. 1998, pp. 273-281.
8. Y. Zhu, W. Zhou, J. Yu, Y. Chen, M. Liu, and Z. Shao, "Enhancing Electrocatalytic Activity of Perovskite Oxides by Tuning Cation Deficiency for Oxygen Reduction and Evolution Reactions," Chemistry of Materials, vol. 28, Feb. 2016, pp. 1691-1697.
9. C. Singh, A. Wagle, and M. Rakesh, "Doped $LaCoO_3$ perovskite with Fe: A catalyst with potential antibacterial activity," Vacuum, vol. 146, Dec. 2017, pp. 468-473.
10. V. Szabo, M. Bassir, A. V. Neste, and S. Kaliaguine, "Perovskite-type oxides synthesized by reactive graining Part IV. Catalytic properties of $LaCo_{1-x}Fe_xO_3$ in methane oxidation," Applied Catalysis B: Environmental, vol. 43, Jun. 2003, pp. 81-92.
11. S. Royer, F. Berube, and S. Kaliaguine, "Effect of the synthesis conditions on the redox and catalytic properties in oxidation reactions of $LaCo_{1-x}Fe_xO_3$," Applied Catalysis A: General, vol. 282, Mar. 2005, pp. 273-284.
12. C. Zhu, A. Nobuta, I. Nakatsugawa, and T. Akiyama, "Solution combustion synthesis of $LaMO_3$ (M = Fe, Co, Mn) perovskite nanoparticles and the measurements of their electrocatalytic properties for air cathode," International Journal of Hydrogen Energy, vol. 38, Oct. 2013, pp. 13238-13248.
13. Z. A. Elsiddig, H. Xu, D. Wang, W. Zhang, X. Guo, Y. Zhang, Z. Sun, and J. Chen, "Modulating Mn^{4+} Ions and Oxygen Vacancies in Nonstoichiometric $LaMnO_3$ Perovskite by a Facile Sol-Gel Method as High-Performance Supercapacitor Electrodes," Electrochimica Acta, vol. 253, Nov. 2017, pp. 422-429.
14. A. Ashok, A. Kumar, R. R. Bhosale, F. Almomani, S. S. Malik, S. Suslov, and F. Tarlochan, "Combustion synthesis of bifunctional $LaMO_3$ (M = Cr, Mn, Fe, Co, Ni) perovskite for oxygen reduction and oxygen evolution reaction in alkaline media," Journal of Electroanalytical Chemistry, vol. 809, Dec. 2017, pp. 22-30.
15. D. Zhang, Y. Song, Z. Du, L. Wang, Y. Li, and J. B. Goodenough, "Active $LaNi_{1-x}Fe_xO_3$ bifunctional catalysts for air cathodes in alkaline media," Journal of Materials Chemistry A, vol. 3, Mar. 2015, pp. 9421-9426.

AUTHORS PROFILE

Shaik Mahammad Rafi, Department of Advanced Materials Engineering, Kongju National University, Cheonan-si, Chungnam 31080, Republic of Korea